COMPDYN 2013
4th ECCOMAS Thematic Conference on
Computational Methods in Structural Dynamics and Earthquake Engineering
M. Papadrakakis, V. Papadopoulos, V. Plevris (eds.)
Kos Island, Greece, 12–14 June 2013

LOCAL AND NON LOCAL APPROACHES FOR SIMULATING CFRP-REINFORCED CONCRETE SHEAR WALLS UNDER MONOTONIC LOADS

K. LE NGUYEN[1]*, M. BRUN[1], A. LIMAM[1], E. FERRIER[2], L.MICHEL[2]

[1]INSA-Lyon, Laboratoire de Génie Civil en Ingénierie Environnementale, Bât. Coulomb, 34 avenue des Arts, 69621, Villeurbanne, France; khuong.le-nguyen@insa-lyon.fr

[2] Université de Lyon 1, Laboratoire de Génie Civil en Ingénierie Environnementale, 82 bd Niels Bohr-69622 Villeurbanne, France

Keywords: Shear wall, Reinforcement with composite, Nonlinear pushover analysis.

Abstract. *In recent years, large efforts from the engineering and scientific communities have been underway for optimizing the behavior of reinforced concrete shear walls of buildings subjected to earthquake loading. The efficiency of shear walls to sustain the earthquake loads mainly depends on the aspect ratio H / L, where H and L are the height and the length of the wall, related to the moment-to-shear ratio M / VL, the vertical load P, and the percentages of vertical and horizontal reinforcements ρ_v and ρ_h. In this paper, two reinforced concrete walls have been experimentally and numerically investigated: the first one, corresponding to the squat wall, with an aspect ratio equal to 0.67, whose behavior is essentially controlled by shear, and the other one with an aspect ratio equal to 2.5, corresponding to the slender wall, whose behavior is governed by both shear and bending. The shear walls are designed for failing with inclined web cracking caused by diagonal tension. Different reinforcement strategies have been considered using CFRP materials. Finite element analyses have been carried out, adopting a plane stress approach with a local concrete model based on the smeared fixed crack approach. The reinforcement and the CFRP materials are provided by bar elements whose nodes are the same as the concrete elements (perfect bond assumption). The experimental and numerical results are compared in terms of the pushover curves (shear strength and ductility) and the cracking patterns.*

1 INTRODUCTION

Reinforced concrete shear walls represent one of the most widespread bracing systems for buildings. Post-earthquake observations surprisingly report good seismic behavior of structural wall buildings [1] while evaluation of existing buildings according to modern standards often concludes that they provide insufficient safety margins [2]. Although reinforced concrete walls are efficient to dissipate the seismic induced energy, they exhibit important damage. The main causes of damage are: occurrence of unpredictable high seismic activity, improper design and construction flaws. The RC wall response behavior depends to a great extent on its height to length ratio. The RC wall characterized by H/L ratio greater than 2 can be considered as slender or long wall, whereas the wall characterized by H/L ratio less than 2 is considered as short wall. Based on experimental works, some analytical models were developed to predict the inelastic strength of walls subjected to reverse cyclic loading and to calculate the natural frequencies of the walls (Mostofinejad D. *and al.* [3], Su and Jon [4], Greifenhagen [5]).

During an earthquake, the shear walls play a major role in resisting lateral loads for tall concrete buildings. They must be carefully designed to provide not only adequate strength, but also sufficient ductility to avoid brittle failure under strong lateral loads. In this context, there are many methods seeking to improve the bearing capacity and the coefficient of ductility with different materials. Current recommendations for the seismic retrofit of RC walls, provided in ASCE 41-06 [6], involve combinations of strengthening and/or ductility enhancement of the critical details by different methods such as the reduction of flexural strength, addition of confinement jackets at wall boundaries or the increase of the shear strength of the wall [7]. In the last decade, composite materials (carbon or glass fibers associated with polymeric matrices CFRP) applied to RC elements by bonding are proved to be effective for the protection and reinforcement of beams and columns. Recent research on reinforced concrete walls strengthened with FRP composites were conducted by Ferrier [8], Antoniades *et al.* [9,10], Demeter *et al.* [11], Dan [12] , El-Sokkary [13], showed the ability to restore the initial performance of the structural members by repairing and strengthening.

Beside experimental testing programs, a better understanding of the structural behavior of the RC wall buildings requires many parametric studies using relevant numerical models. The finite element approach can be employed to model the RC shear walls reinforced by FRP composites and stirrups [3]. In this paper, the finite element code Cast3M is used to model and interpret the behavior of two types of concrete walls reinforced by fiber carbon material. The nonlinear pushover analyses of the shear walls (without FRP and FRP-reinforced) also include the crack patterns and the failure modes.

2 EXPERIMENTAL DATABASE

2.1 Materials

In order to assess the concrete properties, 16x32 cylindrical specimens were cast and tested at 28 days. For the mix of slender walls, the average compressive strength is determined as 34.65 MPa ± 1 MPa. For the mix of short walls, the average compressive strength is 35.93 MPa ± 0MPa. The steels are consistent with the current standard with guaranteed yield strength equal to 500 MPa, the type of steel being S500B. The Freyssinet reinforcement was used. This reinforcement is called CFRP ® with 70% and 30% in each direction. Wicks are used as anchors into the footing of the walls.

Properties	Value
Average thickness	0.48 mm
Ultimate strength	1700 MPa
Module young	105000 MPa
Strength/1cm 1er direction	8.15 kN
Strength/1cm 2er direction	3.5 kN

Table 1: CFRP Material Properties

2.2 Specimen design

The test set-up is shown in the Figure 1. The specimen consists of three parts: the head beam through which the loads are transferred to the panel, the panel corresponding to the shear wall, and the footing at which the specimen is anchored. Uplift of the footing with respect to the laboratory floor is prevented by post-tensioned anchor rods. The test program included two series. The first one included two specimens of the slender type with labels VE1 (without CFRP) and VER1 (reinforced by CFRP). The second included two specimens of short type with labels VC1 (without CFRP) and VCR1 (reinforced by CFRP).

Specimen	l_w (m)	h_w (m)	T (m)	N (kN)
VE1	0.6	1.5	0.08	90
VER1	0.6	1.5	0.08	90
VC1	0.9	0.61	0.08	110
VCR1	0.9	0.61	0.08	110

Table 2: Geometric characteristics of specimens

The monotonic loading was applied by pushing the head beam with a hydraulic cylinder capacity of 500kN. In this case the lateral displacement was imposed at a speed of 0.01 mm/sec. Two post-tensioning bars were used to subject the specimens to axial loading. The bars were located at mid-length of the specimens on both sides of the panel. Before the static test, the bars were alternately post-tensioned in small increments up to the target force with the help of

a hydraulic jack. The vertical post-tensioning force could be maintained at a constant level during the test: 90kN for the slender wall and 110kN for the short wall.

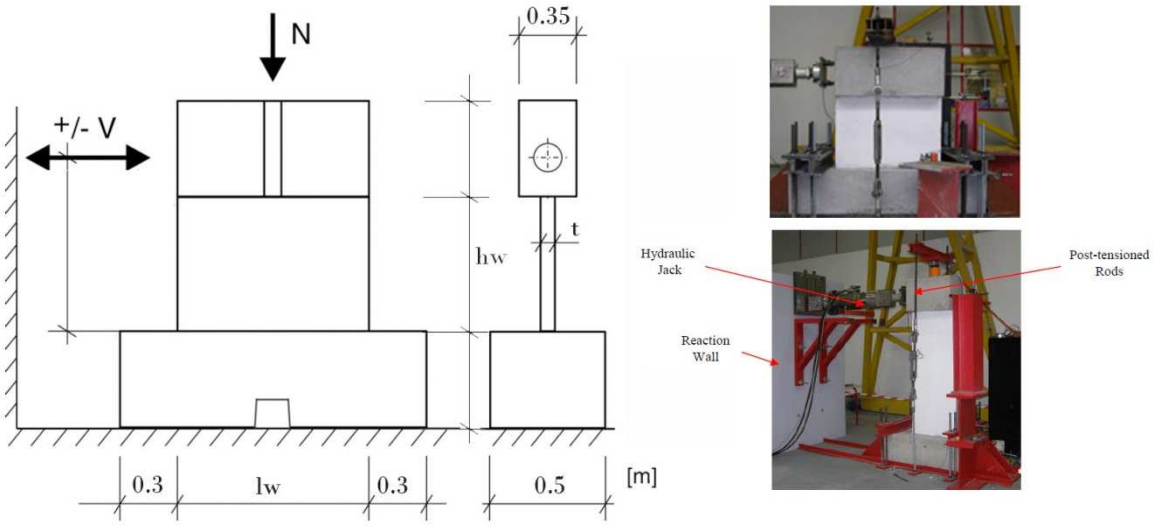

Figure 1: Set-up of the test

The reinforcement is composed of two sheets of wire mesh (Φ 4.5 mm spaced at 200 mm in both directions) and, at each end, of two bars of 6 mm diameter. Rebars of 12mm diameter were used for the reinforcement of the head beam and the footing (Figure 2 and Figure 3). In the case of reinforcement by CFRP, the CFRP 50mm wide bands were used. Three bands over the total height of the wall were applied on each side. The distance between vertical bands is equal to 225mm for the slender wall (VER1) and 230mm for the short wall (VCR1). Seven horizontal bands and four horizontal bands were put in place on each side of VER1 and VCR1, respectively (Figure 4).

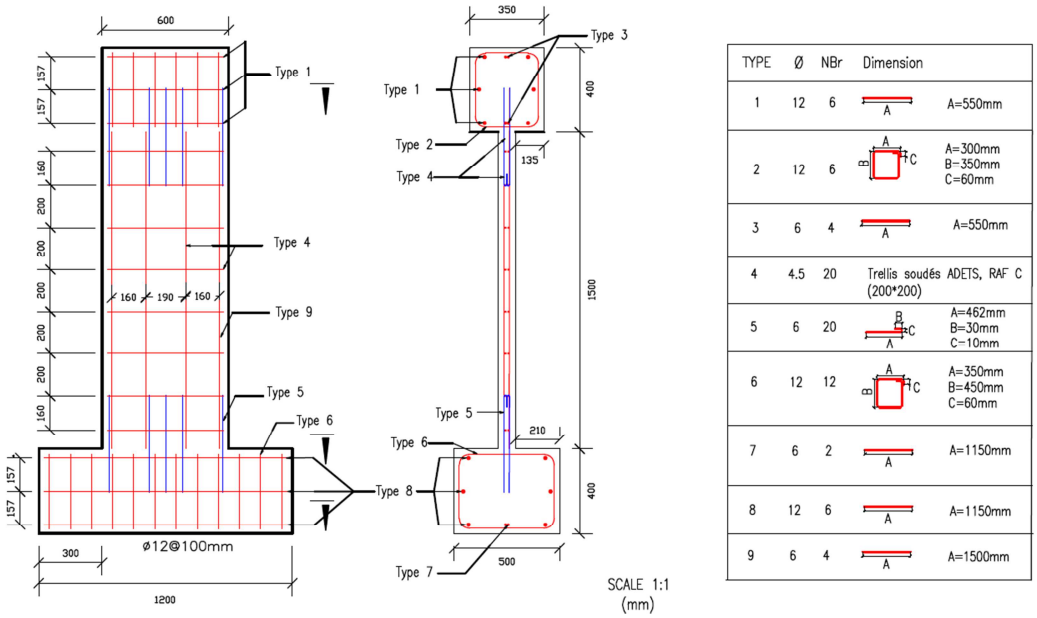

Figure 2: Reinforcement of the slender walls (VE1 and VER1)

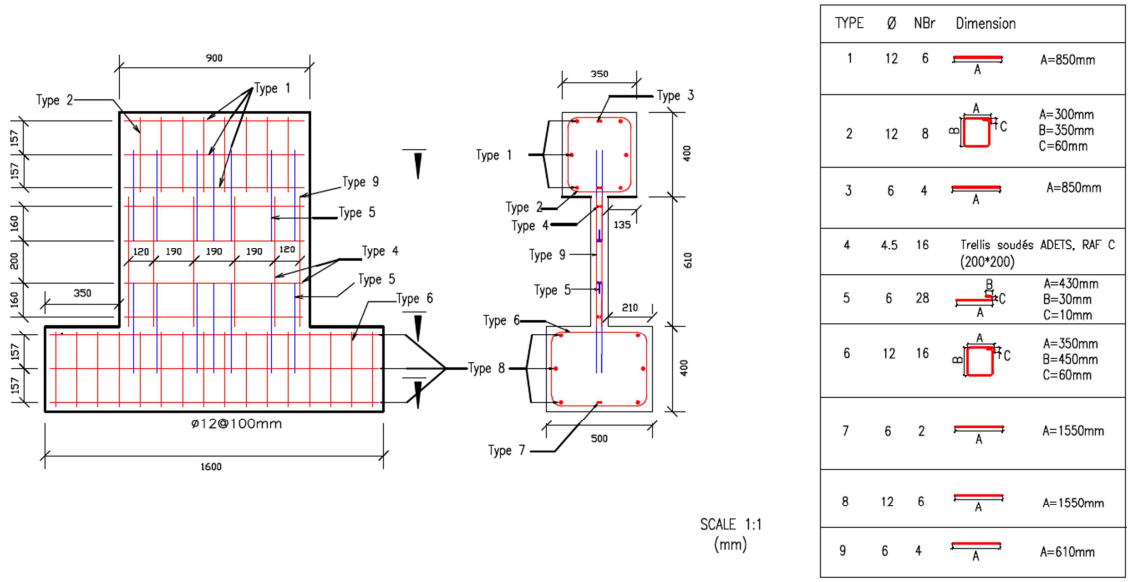

TYPE	Ø	NBr	Dimension	
1	12	6		A=850mm
2	12	8		A=300mm B=350mm C=60mm
3	6	4		A=850mm
4	4.5	16	Trellis soudés ADETS, RAF C (200*200)	
5	6	28		A=430mm B=30mm C=10mm
6	12	16		A=350mm B=450mm C=60mm
7	6	2		A=1550mm
8	12	6		A=1550mm
9	6	4		A=610mm

Figure 3: Reinforcement of the short walls (VC1 and VCR1)

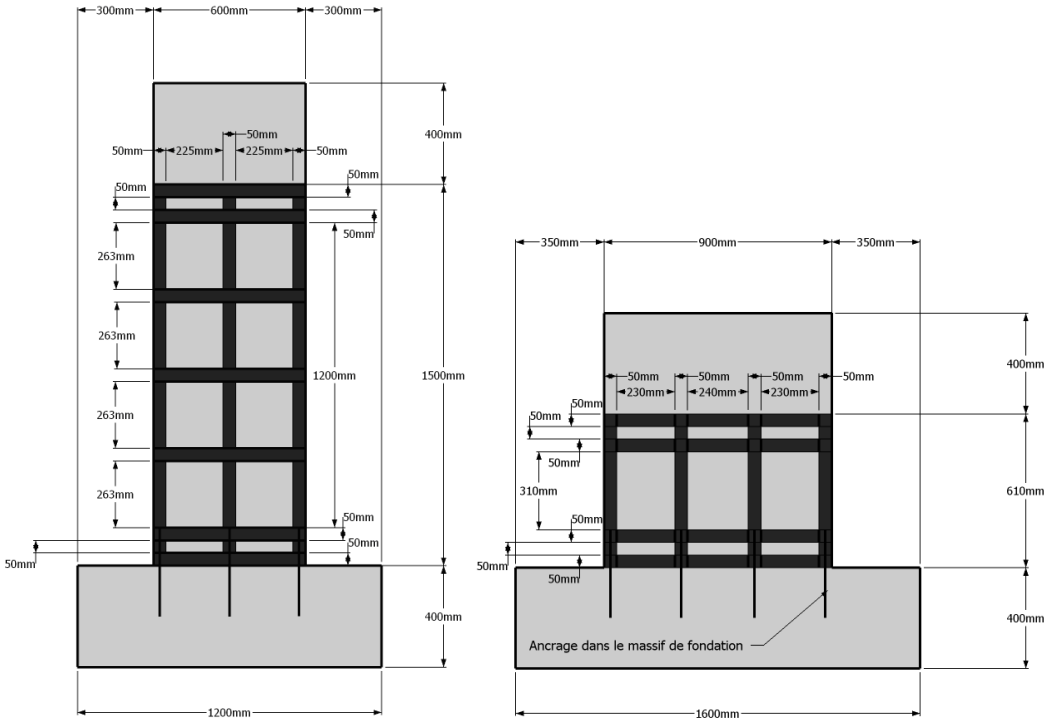

Figure 4: CFRP reinforcement design for VE and VC walls

3 CONSTITUTIVE MODELS FOR FINITE ELEMENT APPROACH

From a general point of view, the concrete is by far one of the most common quasi-brittle materials. It has an asymmetric behavior between tension and compression: weak in tension and ductile in compression, the concrete is a material whose main cause of damage is the cracking.

In the case of compressive cyclic loads, hysteretic phenomena appear as a signature of a sliding friction occurring between the lips of the cracks. All these mechanisms make the behavior of concrete complex to model. In order to evaluate safety margins of reinforced concrete buildings subjected to earthquakes, realistic nonlinear models are needed. With the rapid development of computer technology, considerable research has focused on developing more realistic concrete models for predicting the stress-strain behavior under various load time histories. Several concrete behavior models are implemented into the code Cast3M [14] of CEA. Two types of concrete model are explored: a classical smeared fixed crack approach developed in the LGCIE laboratory of INSA Lyon for cyclic loading and a coupled elasto-plastic damage model proposed by Richard *et al.* [15].

3.1 Smeared fixed crack model (INSA) for concrete

The concrete model INSA, developed at INSA Lyon, implemented into the code Cast3M [14] of CEA, is built in the framework of the theory of plasticity in plane stress. The model is defined by two distinctive behaviors depending whether the concrete is cracked or uncracked.

In its uncracked state, the model is based on the plasticity theory with an isotropic hardening and an associate flow rule. The cracked area is covered by the concept of distributed cracking considering the cracked material as a continuous medium. The crack detection surface in tension follows a Nadai criterion. In compression, load surfaces are of the same Nadai type. The evolution of the load surface to the ultimate load surface in compression follows a positive isotropic hardening. A softening regime occurs with a negative isotropic hardening when reaching the ultimate load surface in compression. The cracking surface in traction as well as the initial and ultimate load surfaces is depicted in the principal stress space in Figure 5.

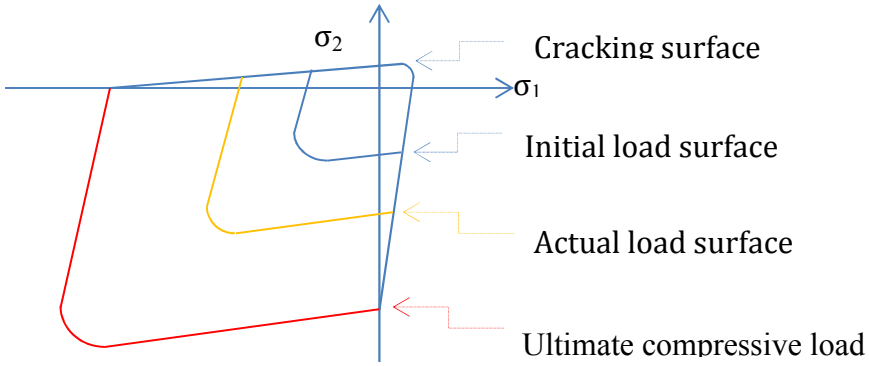

Figure 5: Load surfaces in compression and cracking surface for concrete material

The concrete model enters in its cracked state when the crack detection surface is reached in tension: a fictitious crack is considered perpendicularly to the principal stress direction and its orientation is kept as constant subsequently. A second crack can appear later but only at 90° with respect to the first one. The stress tensor in plane stress assumption is completed by the shear stress, elastically computed using a reduced shear modulus μG; μ parameter corresponds to the classical shear retention factor ($0 \leqslant \mu \leqslant 1$), depending on the crack opening strain for reproducing the loss of shear transfer capability at the crack level. The model's details are presented in [16].

3.2 Damage elasto-plastic (RICRAG) model for concrete

The model RICRAG proposed by Richard *et al.* [15] and available in the code Cast3M is a model for modeling quasi-brittle materials such as concrete in three dimensional. It is a con-

crete model based on isotropic damage mechanics in good agreement with experimental data up to failure; this agreement holds for monotonic loadings as well as for cyclic loadings. Residual strains and hysteretic loops due to friction between the cracks surfaces and elastic stiffness recovery have to be accurately taken into account. The main constitutive equations were formulated within the framework of the thermodynamics for irreversible processes in order to fulfill conservation and evolution principles. Firstly, a consistent state potential is introduced accounting for elasticity, damage, sliding between cracked surfaces and hardenings. Secondly, assuming the positive condition of the intrinsic dissipation rate, state equations can be deduced. Thirdly, complementary equations are introduced to handle the evolution of all the internal variables.

3.3 1D cyclic elasto-plastic model for steels and CFRP bands

The Menegotto-Pinto law [17] represents the behavior of the steels under cyclic loading. The monotonic curve of this law (Figure 6) is characterized by three phases: linear elastic defined by the Young's modulus E_a until the plastic strain σ_{sy},followed by a plateau stress of plastic deformation ε_{sy} at the beginning of the deformation hardening ε_{sh} , and finally a hardening curve until failure. Phases of the monotonic curve are given by:

$$\begin{aligned} &\sigma = E_a.\varepsilon && 0 < \varepsilon < \varepsilon_y \\ &\sigma = \sigma_{sy} && \varepsilon_y < \varepsilon < \varepsilon_{sh} \\ &\sigma = \sigma_{su} - \left(\sigma_{su} - \sigma_{sy}\right).\left(\frac{\varepsilon_{su} - \varepsilon}{\varepsilon_{su} - \varepsilon_{sh}}\right)^4 && \varepsilon \geq \varepsilon_{tm} \end{aligned} \quad (1)$$

where E_a is the elastic modulus of steel, σ_{su} is the ultimate stress and ε_{su} is the ultimate strain of the steel.

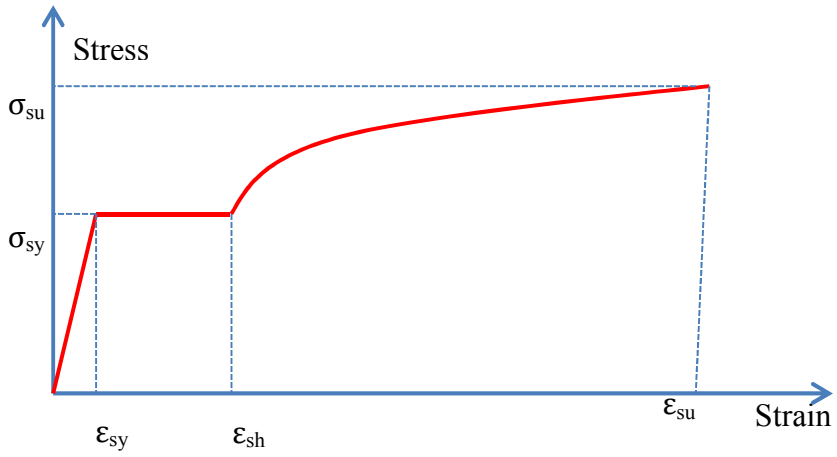

Figure 6: Menegotto-Pinto law under monotonic loading

This model is also used for modeling the CFRP materials.

4 PUSHOVER FINITE ELEMENT ANALYSIS

4.1 Meshes and material properties

The panel, the top beam and the footing were represented either by 2D elements with four nodes with bilinear shape function of displacements or by 3D cube elements with eight nodes.

Steels and CFRP were represented by uniaxial bars. The additional weights were taken into account by applying loads to the top beam as illustrated in Figure 7. The axial compressive load imposed is distributed over a length of 30cm to avoid problems of strain localization. The mesh size of the wall is chosen equal to 2.5cm to connect with steel elements close to the real reinforcement configuration. The adhesion between the steel and concrete materials is assumed to be perfect in this study.

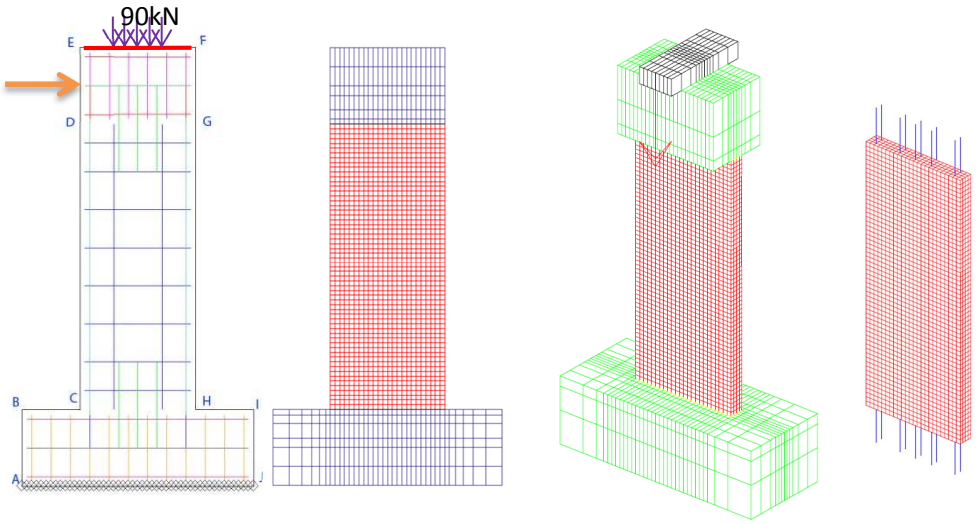

Figure 7: Mesh of the slender wall in 2D and 3D

The compressive loads of 90kN and 110kN are applied for the slender walls and the short walls, respectively. Displacement imposed load is put at the middle of the height of the top beam. The 3D model is shown in Figure 7. We added a rigid element for applying a distributed prior compressive load like in the experimental tests. (Figure 7 and Figure 8)

Table 3 resumes the numbers and the types of elements used in the pushover analyses.

	Approach	Material	Element type	Quantity	Load steps
Slender wall unreinforced by CFRP	2D	Concrete Steel	QUA4 SEG2	1800 864	800
	3D	Concrete Steel	CUB8 SEG2	7200 1728	800
Slender wall reinforced by CFRP	2D	Concrete Steel	QUA4 SEG2	1800 1100	800
	3D	Concrete Steel	CUB8 SEG2	7200 1968	800
Short wall unreinforced by CFRP	2D	Concrete Steel	QUA4 SEG2	4224 1242	700
	3D	Concrete Steel	CUB8 SEG2	18000 2484	700
Short wall reinforced by CFRP	2D	Concrete Steel	QUA4 SEG2	4224 2124	700
	3D	Concrete Steel	CUB8 SEG2	18000 4968	700

Table 3: Numerical approaches

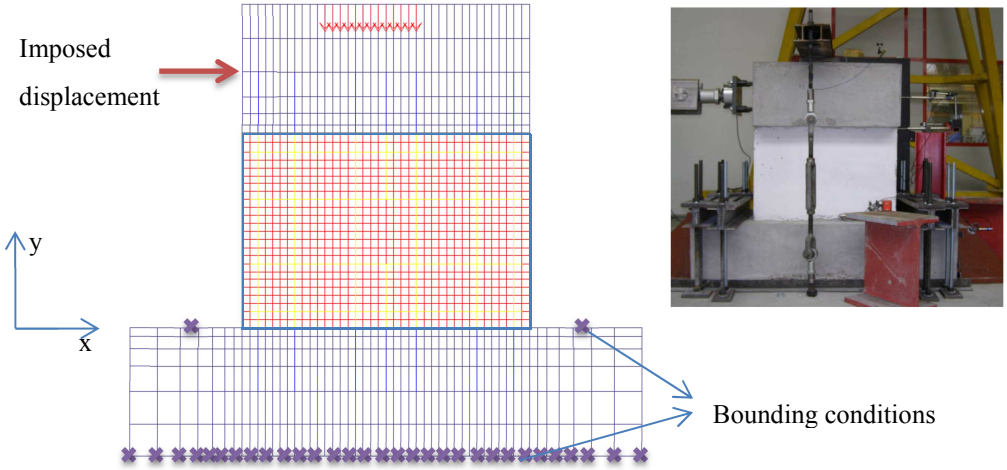

Figure 8: Mesh of the short wall

The parameters of the smeared fixed crack model and the damage elasto-plastic models are reported in Tables 4 and 5.

Symbol	Definition	Short wall	Slender wall
'E'	Young	11.E9 Pa	22.E9 Pa
'FT'	Ultimate stress in simple tension	1.5E6 Pa	1.5E6 Pa
'ALDI'	Brittleness in tension	1.E-2 J.m^3	2.E-2 J.m^3
'ALIN'	Brittleness in compression	5.E-04 J.m^3	10.E-04 J.m^3
'GAM1'	Hardening modulus 1	7.E8 Pa	7.E8 Pa
'A1'	Hardening modulus 2	7.E-07 Pa^{-1}	7.E-07 Pa^{-1}

Tableau 4: Numerical parameters of the model concrete INSA

Symbol	Definition	Short wall	Slender wall
'E'	Young modulus	11.E9 Pa	22.E9 Pa
'LCS'	Ultimate stress in simple compres-	29.E6 Pa	29.E6 Pa
'ALFB'	Stress ratio ultimate tensile	5.E-2	5.E-2
'EPUT'	Ultimate tensile strain	8.E-03	8.E-03
'EMAX'	Fracture strain in compression	1.51E2	1.51E2
'FTC'	Reduction of the shear modulus	5.E-02	5.E-02

Tableau 5: Numerical parameters of the model concrete RICRAG

In the experimental program, it has been observed that the CFRP does not achieve its ultimate strength due to debonding. A maximum strain measured in the CFRP has been assessed as equal to 4500µm/m. Consequently, we assume that the CFRP ultimate tensile strength is equal to 472.5MPa calculated by the formula:

$$\sigma_{rupt} = E_{TFC} \times \varepsilon_{\max} \tag{2}$$

where E_{CFRP} = 105000MPa and ε_{max} = 4500µm/m are identified in the experimental tests. So, we get: σ_{rupt} = 472.5MPa. This hypothesis is used for the short and slender walls.

	E (GPa)	σ_{sy}(MPa)	ε_{sy}	ε_{sh}	σ_{su}(MPa)	ε_{su}
Steel	210	500	2.38E-3	3.5E-3	550	0.05
CFRP	105	472.5	4.5E-3	6E-3	500	0.05

Tableau 6: Parameters of steel and CFRP

To solve the nonlinear equilibrium equations, a modified Newton-Raphson strategy has been adopted [16]. This method essentially uses the same algorithm as the Newton-Raphson process but replaces the tangent stiffness matrix by the initial stiffness matrix corresponding to the previous step of load step. Although the advantage of a quadratic rate of convergence of the Newton-Raphson iteration is lost if the exact tangent stiffness matric is not employed, some of the drawbacks of the classic Newton-Raphson algorithm (*i.e.* initially symmetric tangent stiffness matrix may become nonsysmmetric due to the concrete softening) are avoided. The complete monotonic load-displacement response of slender walls (VE1 and VER1) with this method is 800 load steps for 20mm of displacement. The complete monotonic load-displacement response of short walls (VC1 and VCR1) with this method is 700 load steps for 7mm of displacement. The criterion for convergence was set equal to 10^{-4} of the norm of the residue vector of the unbalanced loads.

4.2 Pushover simulations

For each wall, three pushover analyses were carried out: 2D analysis with the smeared fixed crack concrete model, 2D and 3D with the damage elasto-plastic model.

Slender wall unreinforced: Slender walls are mainly influenced by bending loads and encounter failure either by concrete crushing or yielding of the vertical reinforcement. In addition, it can be due to a combination of both previous mechanisms along with, in some cases, shear slipping of the wall relative to its foundation [18]. During the test on the shear wall VE1, three cracks appeared at a load of 15 kN and a lateral top displacement of 0.9 mm. Then, the yield of longitudinal bar reinforcement is noted at a load of 23.3 kN and a top displacement of 2.8 mm. Finally, the failure occurred due to buckling of the longitudinal bars and concrete spalling at a load and displacement of 25.2kN and 14.2mm, respectively. Figure 9 and Figure 10 show the load-displacement curves and a comparison between the observed mode failures of specimen VE1 in laboratory and the failure modes predicted by the three numerical approaches: 2D INSA concrete model, 2D and 3D RICRAG concrete model. The pushover curves displayed in Figure 9 are in a good agreement. From the failure mode point of view, we can observe that the four major cracks are predicted by the numerical simulation, matching well the experimental results. Each crack is composed of a horizontal crack from the end wall towards the interior of the wall, which is governed by bending, followed by an inclined crack propagating towards the footing, due to shear effects.

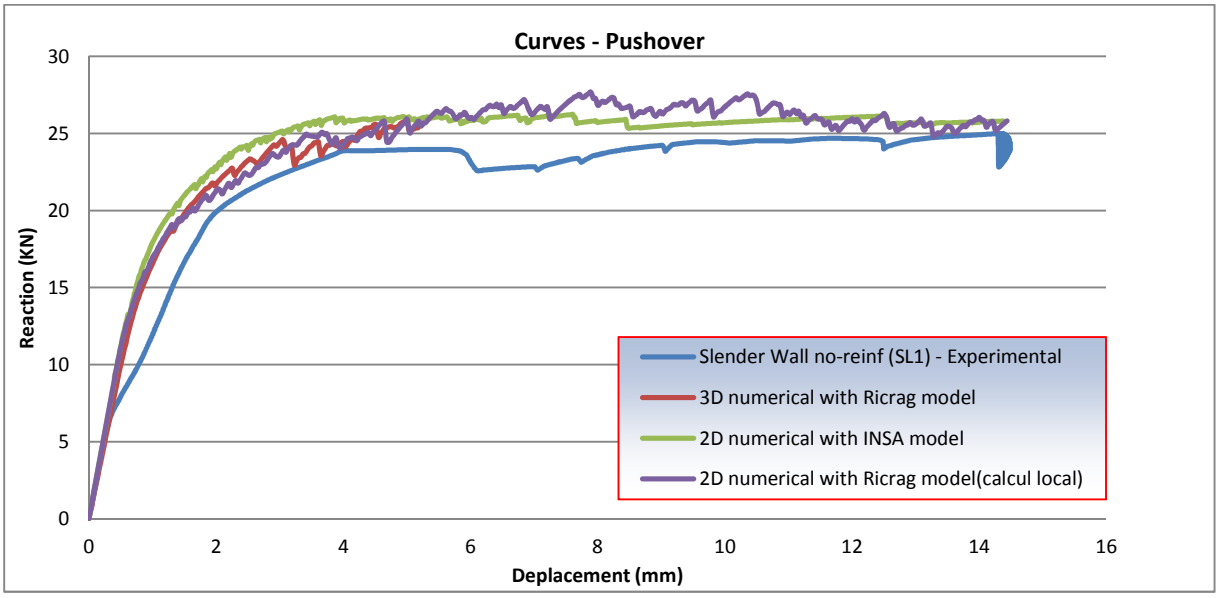

Figure 9: Pushover curves (force-displacement)-slender wall without reinforced

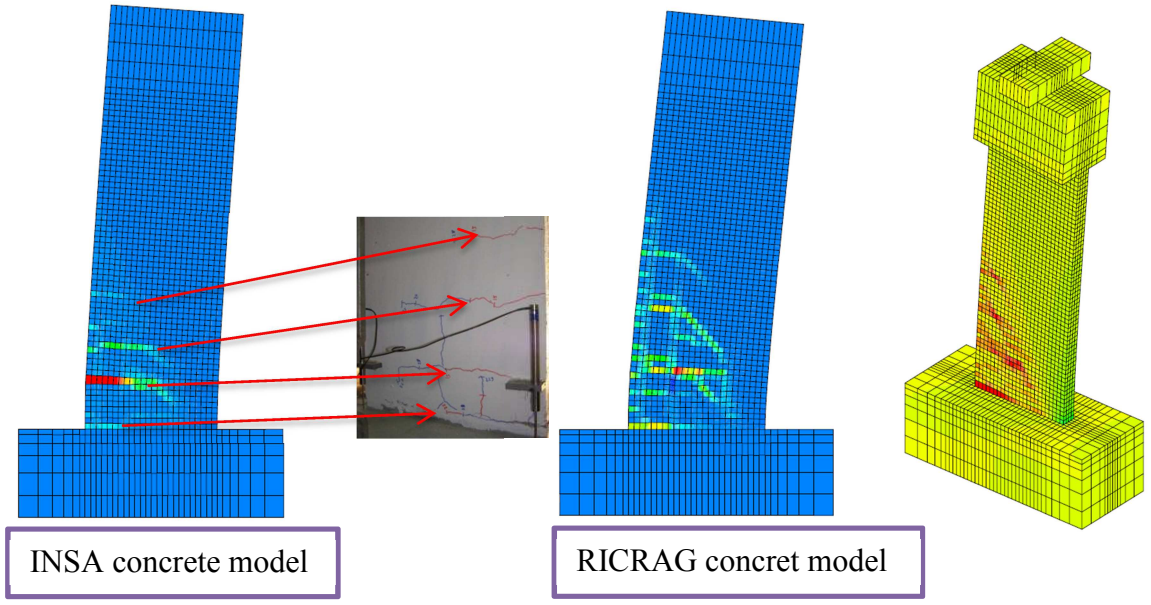

Figure 10: Failure mode – Slender wall unreinforced

Slender wall reinforced with CFRP bands: The mesh of the slender reinforced wall is similar to the one of the previous slender unreinforced wall. All steels and CFRP bands are modeled precisely (Figure 11). Each CFRP band was modeled by three truss-bars having a total section equal to 50x0.48 = 24mm^2. Each wall is reinforced at its footing over a vertical length equal to 250 mm using anchors composed of 26 CFRP threads. In addition, a tissue layer put on the vertical band is added to form a closed layer over the same length of 250 mm. Thus, the truss-bars of a total length of 500 mm were added into the numerical model. The total strength of these three truss-bars modeling a 50mm CFRP band is assessed as equal to 472.5kN.

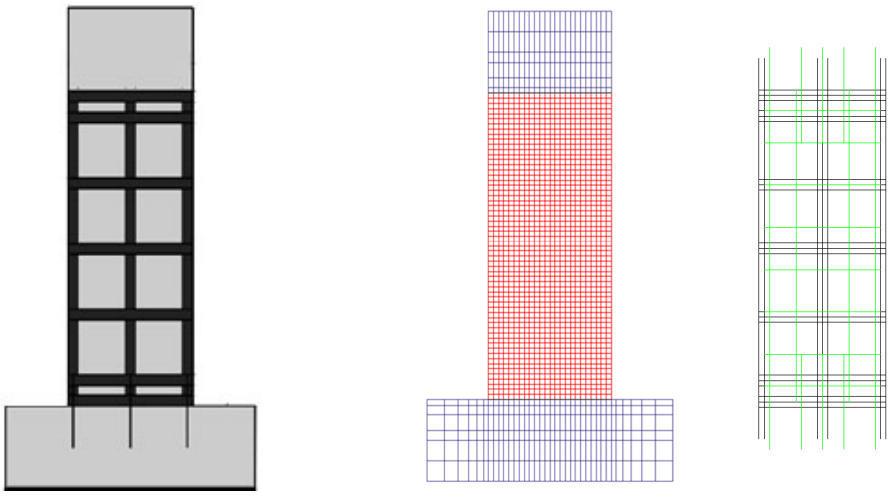

Figure 11: Mesh of the slender wall reinforced by CFRP

Pushover curves were presented in Figure 12, giving a comparison between the numerical results derived from 2D and 3D approaches and the test results. The strengthening with CFRP bands increases the load carrying capacity of the shear wall from 25 kN to 40 kN, that is approximately by 60%. The comparison of curves in Figure 9 and Figure 12 shows that the CFRP layers improves the overall structural behavior of the wall, including both loading capacity and ultimate displacement.

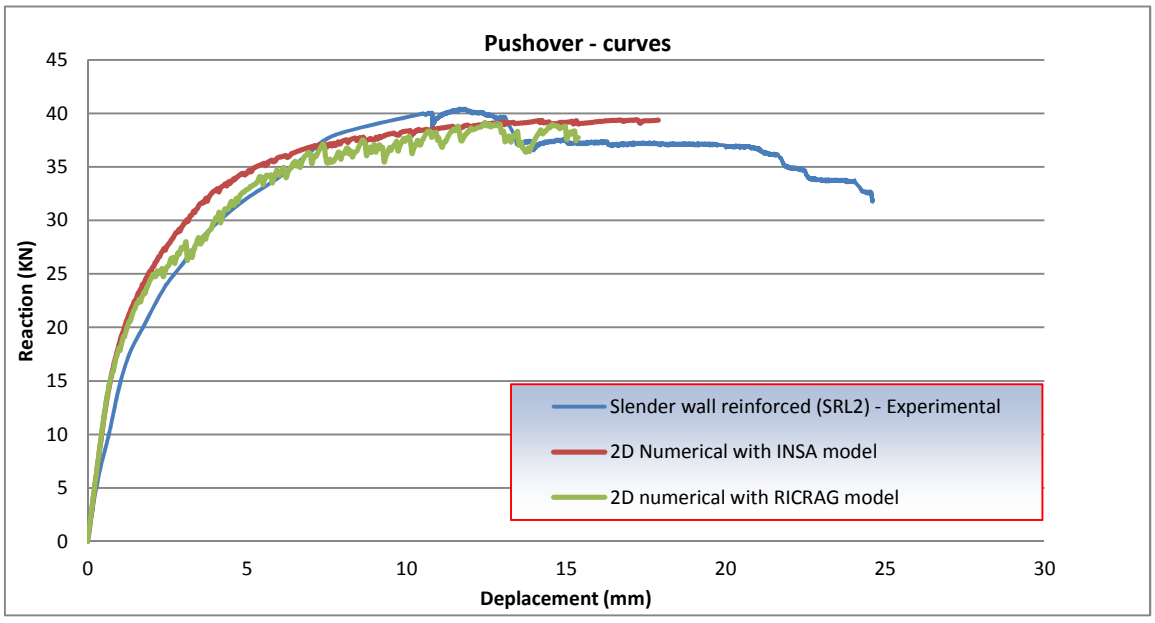

Figure 12: Pushover curves (force-displacement)-slender wall reinforced

The failure modes are displayed in Figure 13 at 20mm of displacement. The cracking patterns at the ultimate load experimentally observed and numerically predicted are compared in Figure 13. The strain localization area indicates the cracked area. It is observed that the numerical model is able to reproduce the cracking pattern along the height of the wall with a good accuracy.

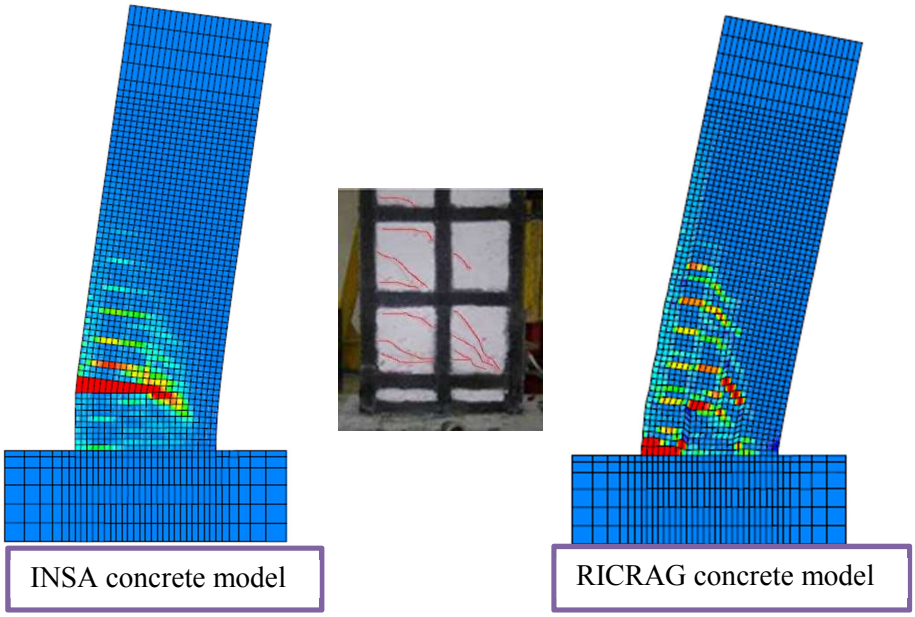

Figure 13: Failure mode – Slender wall reinforced

Short wall unreinforced: This wall constitutes a mixed case because it works in shear and bending. The shear stress cracking develops first in the horizontal direction over a length of 344 mm and then is inclined at an angle of 48° towards the opposite lower bottom corner. On the basis of observations during the experimental tests, we consider that there is a particular area of 35 cm length near the interface between the wall and the top beam. This area is modeled by the same type of concrete constitutive models (INSA or RICRAG concrete models) with a lower tensile stress so as to initiate the first cracking area as observed in the experimental tests. A linear elastic behavior is assumed for the footing.

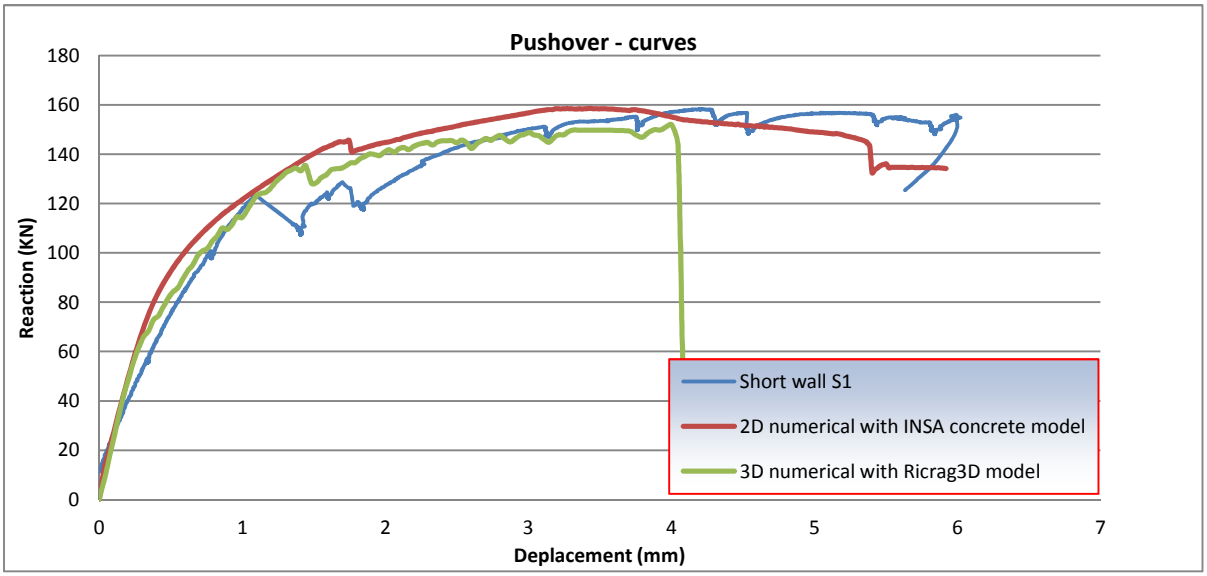

Figure 14: Pushover curves-short wall without reinforced

The results of numerical computations are compared with experimental results in Figure 14. The main failure mode displayed in Figure 15 is a diagonal crack, essentially due to the shear effects. This predicted failure mode is consistent with the experimental cracks observed during the tests and noted elsewhere by Greifenhagen [5] and [18].

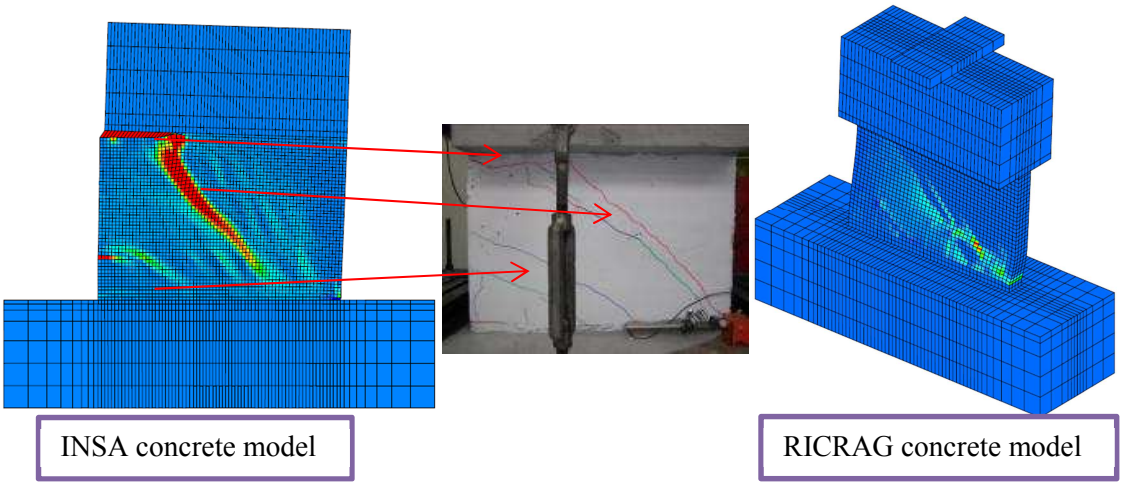

Figure 15: Failure mode of the short wall VC1

Short wall reinforced by CFRP bands: Similar to the modeling of slender wall reinforced by CFRP bands, the truss-bars of 500mm of length were introduced into the numerical model at the bottom of the short wall, with a strength taken as 472.5 kN.

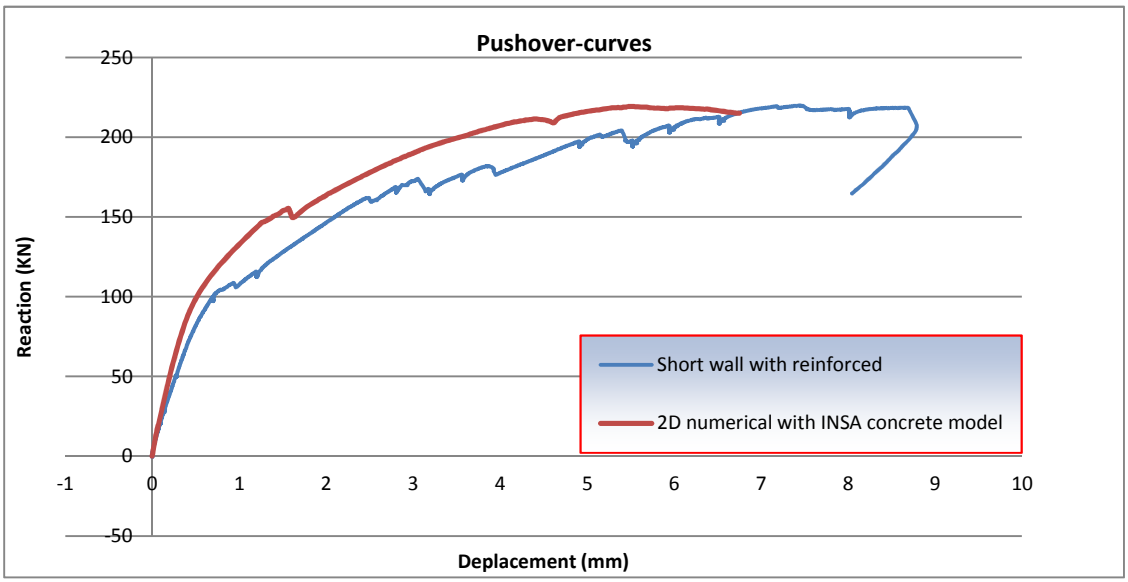

Figure 16: Pushover curves – short wall reinforced

The results in terms of pushover curves show that the model is able to reproduce the nonlinear behavior of the concrete shear wall composed of three phases: the elastic behavior, followed by the crack development and the steel reinforcement hardening. Small differences between the two curves noted in the post-yield region may be due to the imperfect bonding behavior between the concrete and steels, not taken into account in the numerical simulation. The shear strength of the short wall can be limited by both diagonal tension and concrete crushing. The overall deformation of the wall is limited by sliding, concrete crushing, and rupture of reinforcement.

.

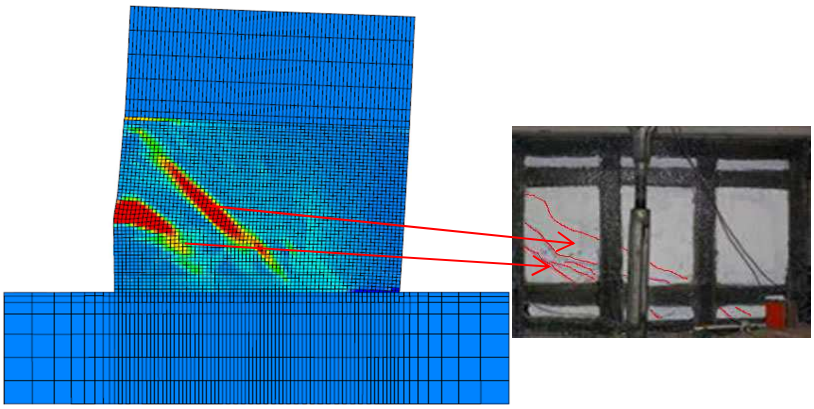

Figure 17: Failure mode of the short wall reinforced

The comparison of experimental and numerical failure modes presented in the Figure 17 exhibits clear similarities with inclined cracks appearing at the border of the wall and propagating towards the footing of the wall.

5 CONCLUSION

The numerical results reproduce the experimental behavior with sufficient accuracy. The numerical model requires a refined and realistic description of the geometry of the wall. Two different concrete models are employed based on either classical smeared fixed crack approach or damage elasto-plastic model. The numerical models are able to predict accurately the shear strength as well as the ultimate displacement and failure modes. It is shown that CFRP bands have to be introduced into the numerical model by considering only a third of his real strength due to the debonding of the bands observed during the experimental tests.

Since the proposed model is only based on limited experimental data, there is an obvious need for further experimental investigations. The present modeling focuses on the static-monotonic behavior of lightly reinforced concrete shear walls. Experimental investigations were made on small-scale test units. Improved modeling should include the static-cyclic behavior and the dynamic behavior. Another important aspect for further research is to study the behavior of the RC walls as a structural elements into a real building. In the present research, the walls were modeled as cantilevers. This assumption merits further investigations in existing building configurations.

REFERENCES

[1] Fintel M., Fintel M. « Performance of buildings with shear walls in earthquakes of the last thirty years ». *PCI journal*. Vol. 40, n°3, p. 62-80.

[2] Iervolino I., Maddaloni G., Cosenza E. « Eurocode 8 Compliant Real Record Sets for Seismic Analysis of Structures ». *Journal of Earthquake Engineering*. 2008. Vol. 12, n°1, p. 54-90.

[3] Mostofinejad D., Mohammadi Anaei M. « Effect of confining of boundary elements of slender RC shear wall by FRP composites and stirrups ». *Engineering Structures*, 2012. Vol. 41, p. 1-13.

[4] Su R. K. L., Wong S. M. « Seismic behaviour of slender reinforced concrete shear walls under high axial load ratio ». *Engineering Structures,* 2007. Vol. 29, n°8, p. 1957-1965.

[5] Greifenhagen C. *seismic behavior of lightly reinforced concrete squat shear walls*. [s.l.] : [s.n.], 2006.

[6] ASCE. *Seismic rehabilitation of existing buildings*. 2007.

[7] Jiang H., Kurama Y. C. « An analytical investigation on the seismic retrofit of older medium-rise reinforced concrete shear walls under lateral loads ». *Engineering Structures*, 2013. Vol. 46, p. 459-470.

[8] Ferrier E. *Mechanical behaviour of concrete wall under static loading*, 2011.

[9] Antoniades K. K., Salonikios T. N., Kappos A. J. « Evaluation of hysteretic response and strength of repaired R/C walls strengthened with FRPs ». *Engineering Structures*. 2007. Vol. 29, n°9, p. 2158-2171.

[10] Antoniades K. K., Salonikios T. N., Kappos A. J. « Tests on Seismically Damaged Reinforced Concrete Walls Repaired and Strengthened Using Fiber-Reinforced Polymers ». *Journal of Composites for Construction*, 2005. Vol. 9, n°3, p. 236-246.

[11] Demeter I. et al. « FRP composites for seismic retrofitting of RC wall panels with cut-out openings ». *Structures & Architecture,* 2010. p. 541-542.

[12] Dan D. « Experimental tests on seismically damaged composite steel concrete walls retrofitted with CFRP composites ». *Engineering Structures*, 2012. Vol. 45, p. 338-348.

[13] El-Sokkary H., El-Sokkary H. « Seismic Retrofit of Reinforced Concrete Shear Walls using Fibre Reinforced Polymer Composites », 2012.

[14] Le Fichoux E. *Présentation Et Utilisation De Cast3m*. CEA, 2011. 92 p.

[15] Richard B., Ragueneu F. « Isotropic continuum damage mechanics for concrete under cyclic loading, : stiffness recovery, inelastic strains and frictional sliding. » *Engineering Fracture Mechanics,* 2010.

[16] Ile N., Reynouard J. . « Nonlinear analysis of reinforced concrete shear wall under Earthquake loading ». *Journal of Earthquake Engineering*. 2000. p. 30.

[17] Menegotto M., Pinto P. *Method of analysis for cyclically loaded reinforced concrete plane frames including changes in geometry and non-elastic behaviour of elements under combined normal force and bending.* 1973.

[18] Greifenhagen C., Lestuzzi P. « Static cyclic tests on lightly reinforced concrete shear walls ». *Engineering Structures*, 2005. Vol. 27, n°11, p. 1703-1712.